# Glucocorticoid-induced alterations in mitochondrial membrane properties and respiration in childhood acute lymphoblastic leukemia ☆

Karin Eberhart [a,c], Johannes Rainer [b,c], Daniel Bindreither [b], Ireen Ritter [a], Erich Gnaiger [d], Reinhard Kofler [b,c], Peter J. Oefner [a], Kathrin Renner [a,*]

[a] Institute of Functional Genomics, University of Regensburg, Josef-Engert-Str. 9, 93053 Regensburg, Germany
[b] Division of Molecular Pathophysiology, Biocenter, Medical University of Innsbruck, Innrain 52, 6020 Innsbruck, Austria
[c] Tyrolean Cancer Research Institute, Innrain 66, 6020 Innsbruck, Austria
[d] D. Swarovski Research Laboratory, Department of Visceral, Transplant and Thoracic Surgery, Innrain 66, 6020 Innsbruck, Austria

## ABSTRACT

Mitochondria are signal-integrating organelles involved in cell death induction. Mitochondrial alterations and reduction in energy metabolism have been previously reported in the context of glucocorticoid (GC)-triggered apoptosis, although the mechanism is not yet clarified. We analyzed mitochondrial function in a GC-sensitive precursor B-cell acute lymphoblastic leukemia (ALL) model as well as in GC-sensitive and GC-resistant T-ALL model systems. Respiratory activity was preserved in intact GC-sensitive cells up to 24 h under treatment with 100 nM dexamethasone before depression of mitochondrial respiration occurred. Severe repression of mitochondrial respiratory function was observed after permeabilization of the cell membrane and provision of exogenous substrates. Several mitochondrial metabolite and protein transporters and two subunits of the ATP synthase were downregulated in the T-ALL and in the precursor B-ALL model at the gene expression level under dexamethasone treatment. These data could partly be confirmed in ALL lymphoblasts from patients, dependent on the molecular abnormality in the ALL cells. GC-resistant cell lines did not show any of these defects after dexamethasone treatment. In conclusion, in GC-sensitive ALL cells, dexamethasone induces changes in membrane properties that together with the reduced expression of mitochondrial transporters of substrates and proteins may lead to repressed mitochondrial respiratory activity and lower ATP levels that contribute to GC-induced apoptosis. This article is part of a Special Issue entitled: Bioenergetics of Cancer.

© 2010 Elsevier B.V. All rights reserved.

## 1. Introduction

Mitochondria are involved in many vital metabolic pathways, e.g. citric acid cycle (TCA), energy transformation, amino acid metabolism, and urea cycle. This is reflected in their complex architecture and the high number of metabolite transport systems [1,2] tightly controlled by membrane potential (electrogenic substrate transport), proton gradients (protonogenic substrate transport), and substrate gradients, including the gradient of inorganic phosphate, $P_i$. Although mitochondria possess their own genome, they mainly depend on import of proteins, synthesized by cytoplasmic ribosomes and imported via mitochondrial protein translocases. Translocases of the outer mitochondrial membrane (TOMM) and inner mitochondrial membrane (TIMM) facilitate protein uptake and insertion. A disturbed transport of newly synthesized proteins into mitochondria can impair growth,

cell proliferation, and respiration of affected cells [3]. Mitochondria are important death signal integrators and key organelles involved in the onset of the intrinsic apoptotic pathway [4,5]. Membrane alterations, reduction of mitochondrial membrane potential, and release of pro-apoptotic proteins, such as cytochrome $c$ and apoptosis inducing factor (AIF), are well described events of this apoptotic pathway, induced by a variety of cell death stimuli. Because of their ability to induce cell cycle arrest and cell death, glucocorticoids (GC) are exploited in the therapy of lymphoid malignancies, particularly in childhood acute lymphoblastic leukemia (ALL) [6,7]. Despite a high cure rate (75%), severe therapy related side effects, resistance development, and relapses are frequently observed.

Besides proteins of the Bcl-2 family, metabolic alterations are involved in GC-induced apoptosis [8]. Reduction in cellular glucose uptake, lactate production, and ATP content have been described recently [9,10]. Conversely, upregulation of important metabolic pathways including glycolysis, oxidative phosphorylation, glutamate metabolism, and cholesterol biosynthesis at the transcriptional level have been related to GC resistance [11]. Nevertheless, the complex pattern of GC-induced mitochondrial alterations and their involvement

in cell death and resistance warrant further investigations to improve therapy protocols and revert GC resistance.

In a previous study, we investigated the time response of respiratory activity under treatment with dexamethasone (DEX) in intact cells and showed preserved ROUTINE respiration and capacity of the electron transport system (ETS) up to 24 h of treatment but a significant reduction after 36 h [9]. To gain more insight into GC-induced mitochondrial alterations, we measured mitochondrial respiratory activity in detail in GC-sensitive and resistant cell lines by high-resolution respirometry. Mitochondrial respiratory capacity was analyzed after cell membrane permeabilization with digitonin and addition of substrates feeding electrons into complex I (CI) and complex II (CII) separately or simultaneously. DEX treatment resulted in repressed mitochondrial activity in GC-sensitive but not in GC-resistant cells. Furthermore, we frequently detected cytochrome $c$ release in one model system. These results together with the finding that a variety of mitochondrial transporters involved in metabolite transport and protein uptake were downregulated at the mRNA level indicate changes in mitochondrial membrane properties in the course of GC-induced cell death in ALL.

## 2. Materials and methods

### 2.1. Cell culture

The GC-sensitive cell lines CCRF-CEM-C7H2 [12], NALM-6 (ACC 128, DSMZ), and 697/EU-3 ALL [13], and the GC-resistant cell lines CEM-C7H2-R9C10 and CEM-C7H2-R1C57 [14] were used as ALL model systems. The original name of the cell line 697/EU-3 given by its generator was "line 697," but it was renamed recently EU-3 [15]. Cells were maintained in RPMI 1640 supplemented with 10% heat-inactivated tetracycline-free fetal calf serum, 2 mM L-glutamine (all PAA; Pasching, Austria) in a humidified atmosphere of 95% air and 5% $CO_2$ at 37 °C. All cell lines were regularly tested for mycoplasma contamination (Minerva Biolabs, Berlin, Germany) and were found to be negative.

### 2.2. Induction and determination of apoptosis

Cells were diluted to $3 \times 10^5$ cells/mL and incubated with 100 nM DEX (Sigma-Aldrich, St. Louis, MO, USA). Control cells were treated with carrier only, i.e. 0.1% (vol./vol.) ethanol. Apoptosis was determined by flow cytometric analysis (Beckman Coulter, Krefeld, Germany) of the sub-G1 fraction after DNA staining according to Nicoletti [16].

### 2.3. Cell number and protein determination

Cell numbers and volumes were analyzed by means of a CASY1 TT cell counter (Schärfe System, Reutlingen, Germany). Protein content was measured in the presence of a protease inhibitor (Pierce, Rockford, IL, USA) using the Coomassie Plus Protein Assay Reagent Kit (Pierce) with bovine serum albumin as standard.

### 2.4. ATP quantification

Intracellular ATP levels were measured in freshly harvested cells by a luminescence assay (Promega, Madison, WI, USA). The emitted light was proportional to the ATP concentration. An ATP standard curve was generated to quantify cellular ATP according to the manufacturer's protocol.

### 2.5. Cell fractionation

Approximately $6 \times 10^7$ cells were harvested, washed with cold PBS 3 times, resuspended in 1 mL mitochondria isolation buffer (10 mM HEPES, pH 7.4, 0.25 M sucrose, 1 mM EDTA, 0.1 mM phenylmethyl-sulfonylfluoride, 1 mM sodium fluoride, 0.2 mM sodium vanadate), and centrifuged at 500g for 2 min at 4 °C. The supernatant was discarded and the pellet was resuspended in 1 mL of isolation buffer. The cells were mechanically disrupted by 20 strokes in a glass/Teflon potter and fractions were separated by differential centrifugation (500g for 2 min, 1,500g for 10 min, 12,000g for 10 min, all at 4 °C) to obtain the mitochondria-enriched fraction.

### 2.6. High-resolution respirometry

Activity of the respiratory system was analyzed in a two-channel titration injection respirometer (Oxygraph-2k; Oroboros Instruments, Innsbruck, Austria) at 37 °C. Cells were harvested, resuspended in mitochondrial medium MiR05 [17], and transferred to the oxygraph chambers at final cell densities of approximately $1 \times 10^6$ cells per milliliter. In the first substrate-uncoupler-inhibitor titration (SUIT) protocol (Fig. 1A and B), ROUTINE respiration (no additions), LEAK respiration (oligomycin-inhibited, 2 µg/mL), and ETS capacity (maximum non-coupled respiration induced by stepwise (typically 2–3 steps) titration of carbonyl cyanide p-(trifluoromethoxy) phe-nylhydrazone (FCCP; 2 µM solved in ethanol)) were measured in intact cells respiring on endogenous substrates. Subsequently, the plasma membrane was permeabilized with digitonin (8.1 µM), and CI-dependent ETS capacity ($CI_{ETS}$) was stimulated by glutamate (G; 10 mM) and malate (M; 2 mM) addition (5 mM pyruvate did not result in a further increase in respiration, data not shown). After addition of succinate (S; 10 mM), ETS capacity was obtained with convergent CI + II electron flow into the Q-junction ($ETS_{CI + II}$) [18]. Subsequent addition of rotenone (Rot; 0.5 µM) allowed the determination of CII supported ETS capacity ($CII_{ETS}$). Residual oxygen consumption (ROX) was evaluated after inhibition of CIII with antimycin A (Ama; 2.5 µM). In a second SUIT protocol (Fig. 1C and D), after determination of ROUTINE respiration, the plasma membrane was permeabilized with digitonin and the capacity of oxidative phosphorylation (OXPHOS) with CI-related substrates (G + M) was determined after stimulation by ADP (D; 2.5 mM; $CI_{OXPHOS}$), followed by addition of S (CI + $II_{OXPHOS}$). In the next step, ETS capacity was measured by uncoupling with FCCP (CI + $II_{ETS}$). Finally, $CII_{ETS}$ and ROX were determined as in the first protocol. Integrity of the outer mitochondrial membrane was checked by the addition of cytochrome $c$ (10 µM) to CI respiration in both protocols. The absence of a stimulatory effect of cytochrome $c$ on respiration was used as a positive test for integrity of the outer mitochondrial membrane [19]. For further details on SUIT protocols, see reference 20.

### 2.7. Immunoblotting

Proteins of the mitochondria-enriched fractions were size-fractionated by SDS–PAGE, blotted on PVDF membranes (Millipore, Billerica, MA, USA), blocked with 5% skim milk in 10 mM Tris Buffered Saline Tween 20 (TBST) buffer, and incubated with rabbit polyclonal anti-TOMM40 (Santa Cruz Biotechnology, Santa Cruz, CA, USA; diluted 1:500 in 5% skim milk in TBST), mouse monoclonal anti-TIMM8A (Abcam, Cambridge, UK; diluted 1:1000 in 5% skim milk in TBST), and rabbit monoclonal anti-COXIV (Cell Signaling Technology, Danvers, MA, USA; diluted 1:1000 in 5% skim milk in TBST) antibodies. Horseradish peroxidase conjugated secondary antibodies (GE Health-care, Buckinghamshire, UK; diluted 1:2500 in 5% skim milk in TBST) were visualized by an enhanced chemiluminescence reagent (ECL Plus, Amersham, Uppsala, Sweden) and detected by the Molecular Imager® VersaDoc™ MP 4000 system (Bio-Rad Laboratories Inc., Hercules, CA, USA). Single bands were analyzed densitometrically using the Quantity One Software (Bio-Rad Laboratories). TIMM8A and TOMM40 bands were normalized against the mitochondrial loading control COXIV.
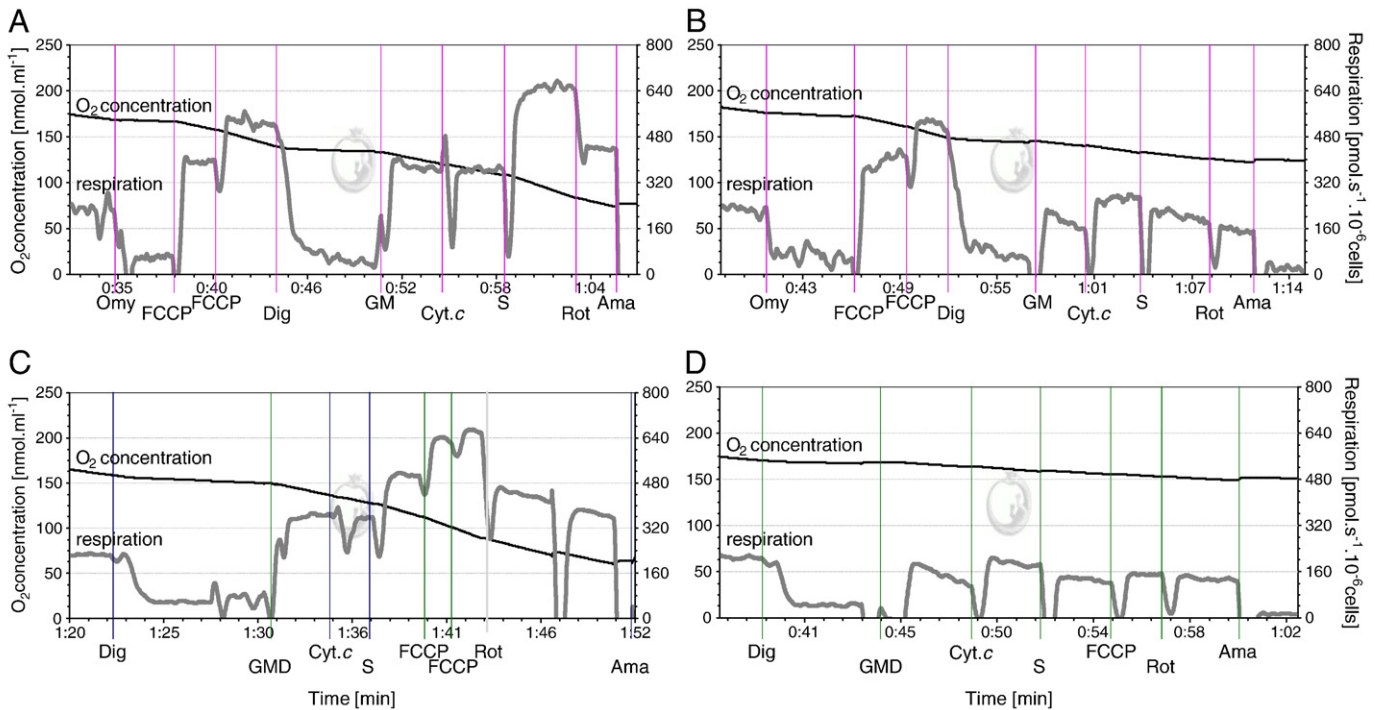
**Fig. 1.** Online high-resolution respirometry traces of mitochondrial respiration in representative experiments with two protocols applied to control (A,C) and DEX-treated (B,D) C7H2 cells after 24 h of incubation. Titrations (A and B): ROUTINE respiration (intact cells in MiR05), oligomycin (Omy; LEAK respiration), FCCP (2 steps; ETS capacity), digitonin (Dig), glutamate + malate (GM; CI$_{ETS}$), cytochrome c (Cyt c), succinate (S; CI + II$_{ETS}$), rotenone (Rot; CII$_{ETS}$), antimycin A (Ama; ROX). In A and B, respiration was uncoupled with FCCP in intact cells and, subsequently, the cell membrane was permeabilized. Titrations (C and D): ROUTINE respiration, Dig, G, M, and ADP (CI$_{OXPHOS}$), Cyt c, S (CI + II$_{OXPHOS}$), FCCP titration (CI + II$_{ETS}$), Rot (CII$_{ETS}$), Ama (ROX). Vertical lines indicate titrations. Respiration was reduced in permeabilized cells in both protocols.

## 2.8. Microarray analysis

Generation of the Affymetrix Exon microarray (HuEx-1.0-st v2) data sets have been published ([21] and Rainer et al., in preparation). In brief, total RNA from GC-sensitive ALL cell lines CCRF-CEM-C7H2, 697/EU-3, and NALM-6, which had been cultured in the presence and absence of 100 nM DEX, respectively, were hybridized to Exon microarrays using standard protocols. Raw microarray data were preprocessed using the GCRMA algorithm [22]. P-values for significance of differential expression were calculated using the moderated t-test [23] and adjusted for multiple hypothesis testing using the method by Benjamini and Hochberg [24].

The characteristics of 27 childhood ALL patients (7 T-ALL and 20 precursor B-ALL patients) and the generation of their gene expression profiles during systemic GC monotherapy has been described previously ([25] and Rainer et al., in preparation). In brief, total RNA was extracted from Ficoll-purified and MACS-sorted (if blast counts were below 80%) peripheral lymphoblasts of childhood ALL patients prior to and 24 h after initiation of GC therapy following the BFM (Berlin–Frankfurt–Münster) therapy protocol recommendations, converted into labeled targets, and hybridized to Affymetrix HGU133 Plus 2.0 GeneChips according to the manufacturer's standard protocols. Microarrays were preprocessed using the GCRMA method.

## 3. Results

### 3.1. Determination of apoptosis and protein content under GC treatment

Cells were treated with 100 nM DEX, a concentration chosen with regard to its clinical relevance. After 24 h of DEX treatment, the apoptotic rates of both the CCRF-CEM-C7H2 and the 697/EU-3 cell line were comparable to controls (7% ± 2%) as measured by sub-G1 peak detection. Cell death kinetics differed between the two cell lines. About 27% ± 5% of the C7H2 cells were apoptotic after 36 h, whereas in the case of 697/EU-3, apoptotic cells were first detected after 48 h (13% ± 4%). In CEM-CCRF-C7H2 cells also, protein content changed significantly after 24 h (control, 0.144 ± 0.009 mg/10$^6$ cells; DEX, 0.118 ± 0.008 mg/10$^6$ cells*, P<0.05) and after 36 h (control, 0.125 ± 0.009; DEX, 0.089 ± 0.008 mg/10$^6$ cells*, P<0.05) of treatment. In 697/EU-3 cells, protein content was slightly decreased after 24 h (control, 0.098 ± 0.008 mg/10$^6$ cells; DEX, 0.082 ± 0.005 mg/10$^6$ cells) and was unchanged after 36 h (control, 0.097 ± 0.01 mg/10$^6$ cells; DEX, 0.105 ± 0.011 mg/10$^6$ cells) of treatment. All respiratory data in this study were already corrected for alterations in cell size.

### 3.2. Mitochondrial respiratory capacity

We analyzed mitochondrial respiratory capacity in two GC-sensitive model systems for acute lymphoblastic childhood leukemia, the CCRF-CEM-C7H2 cell line as a T-ALL and the 697/EU-3 cell line as a precursor B-ALL model, and two GC-resistant cell lines, the CEM-C7H2-R9C10 and CEM-C7H2-R1C57 cells. Since we were interested in events prior to cell death, we investigated mitochondrial function in detail already after 24 h of treatment with carrier only or 100 nM DEX. We applied two different respirometric protocols (see section 2.6), adapted from Gnaiger [18], to gain insight into mitochondrial respiratory function. We found a remarkable difference between the two model systems in their characteristics of the respiratory systems in controls. Whereas ROUTINE respiration was quite similar in the two model systems (Table 1), ETS and OXPHOS capacity was significantly lower in the B-ALL cells (Fig. 2). CI + II supported respiration was highly sensitive to uncoupling, as seen by the increase in ETS capacity versus OXPHOS capacity in the presence of the GMS substrate combination (Fig. 2), showing a substantial limitation by the phosphorylation system.

The DEX effect was comparable for the two GC-sensitive cell lines, although it was more pronounced in the T-ALL model. After 24 h of incubation, ROUTINE respiration and non-coupled ETS capacity on

**Table 1**
Mitochondrial ROUTINE respiration and ETS capacity in intact cells and ATP levels after 24 and 36 h of treatment with carrier (0.1% ethanol; C) and 100 nM dexamethasone (DEX), respectively, in C7H2 T-ALL cells and 697/EU-3 preB-ALL cells.

| | | ROUTINE [pmol s$^{-1}$ mg$^{-1}$] | ETS [pmol s$^{-1}$ mg$^{-1}$] | ATP [nmol mg$^{-1}$] |
|---|---|---|---|---|
| *C7H2* | | | | |
| 24 h | C | 216 ± 6 | 468 ± 35 | 43 ± 0 |
| | DEX | 211 ± 4 | 466 ± 36 | 42 ± 1 |
| 36 h | C | 214 ± 5 | 534 ± 5 | 49 ± 1 |
| | DEX | 157 ± 5*** | 369 ± 29* | 41 ± 1** |
| | | | | |
| *697/EU-3* | | | | |
| 24 h | C | 187 ± 6 | 305 ± 13 | 39 ± 2 |
| | DEX | 171 ± 15 | 219 ± 46 | 40 ± 2 |
| 36 h | C | 189 ± 9 | 327 ± 42 | 42 ± 6 |
| | DEX | 117 ± 12*** | 171 ± 52 | 28 ± 3* |

ROUTINE respiratory activity at physiological levels of coupling and ETS capacity in the non-coupled state were measured in intact cells by high-resolution respirometry and related to cellular protein content. ATP concentrations [ATP] were measured in viable cells. Arithmetic means ± SEM and statistical significance compared to controls. $N = 7$.
* $P < 0.05$.
** $P < 0.01$.
*** $P < 0.001$.

endogenous substrates in intact cells did not differ between controls and DEX-treated cells (Table 1). Coupling was not significantly altered, as indicated by the preserved LEAK/ETS control ratio



**Fig. 2.** Reduction of respiration after 24 h of treatment with 100 nM DEX in permeabilized CEM-CCRF-C7H2 (A) and 697/EU-3 cells (B), respectively, respiring on exogenous substrates. Respiratory states are CI$_{OXPHOS}$: 10 mM glutamate + 2 mM malate (GM) and 2.5 mM ADP (D). CI$_{ETS}$: GM, non-coupled state with FCCP. CII$_{ETS}$: 10 mM succinate (S), inhibition of CI by rotenone (0.5 µM), non-coupled state with FCCP. CI + II$_{OXPHOS}$: GMS + D. ETS$_{CI + II}$: GMS + FCCP. Arithmetic means ± SEM and statistical significance compared to controls (*$P < 0.05$, **$P < 0.01$, ***$P < 0.001$); $N = 5$.

(oligomycin-inhibited relative to non-coupled respiration) shown previously [9]. Subsequent permeabilization of the plasma membrane and addition of CI- and CII-related substrates resulted in reduced oxygen consumption under DEX treatment (Fig. 1B). In both models, CI$_{ETS}$ and CII$_{ETS}$ were reduced, as well as ETS capacity supported by CI- and CII-related substrates simultaneously (Fig. 2). Convergent electron input in the ETS increased respiration in control cells compared to separate supply of CI- or CII-substrates. Treatment with DEX not only abolished the stimulatory effect of the addition of succinate to CI substrate-supported respiration (Fig. 1B and D, Fig. 2A and B) but also decreased respiratory activity in some experiments. The lack of stimulation by providing CI and CII-substrates simultaneously cannot be explained by a complete loss of CII function because there was still respiratory activity after rotenone addition (Fig. 2).

A reduction in OXPHOS was detected in both model systems but was statistically significant only in the CEM-CCRF-C7H2 cell line. 697/EU-3 cells were very sensitive to lowering the membrane potential by uncoupling with FCCP prior to permeabilization. The effects on respiratory parameters were much more pronounced in the non-coupled state.

In experiments with DEX-treated CEM-CCRF-C7H2 cells, we frequently detected a decline in respiration over time after digitonin permeabilization of the plasma membrane. The addition of cytochrome *c* stabilized and increased CI respiration, as shown in Fig. 1B and D. This effect was not observed in 697/EU-3 (data not shown). Since in intact cells, ROUTINE respiration and ETS capacity were unchanged after 24 h of DEX treatment compared to control cells, we concluded that cytochrome *c* release was induced after cell membrane permeabilization. After 36 h of DEX treatment, a repression was also detectable in ROUTINE respiration and ETS capacity of intact cells. Moreover, ATP levels were significantly reduced in both model systems (Table 1). Mitochondrial content was not changed by DEX treatment, as shown by a preserved citrate synthase activity in the T-ALL model system, whereas citrate synthase activity in 697/EU-3 cells was significantly decreased [9]. We also investigated two GC-resistant cell lines, namely CCRF-CEM-C7H2 R1C57 and R9C10. We did not detect any of the described treatment related changes in the GC-resistant cell lines as observed in GC-sensitive model systems (Table S1).

### 3.3. Gene expression of mitochondrial transporters

Analysis of the transcriptome after 24 h of treatment with DEX revealed repression of important mitochondrial transport systems, suggesting multiple changes in the mitochondrial membrane composition possibly involved in cell death.

#### 3.3.1. Mitochondrial metabolite transporters

Based on gene expression array data, we found several mitochondrial transporters of the SLC25A family to be significantly repressed under DEX treatment in the ALL model systems CCRF-CEM-C7H2 and 697/EU-3, as well as in another childhood precursor B-ALL model (NALM-6) (Table 2). The mitochondrial glutamate/H+ symporter SLC25A22 (MIM 609302) and the dicarboxylate carrier SLC25A10 (MIM 606794), which transports dicarboxylates such as malate and succinate across the mitochondrial membrane in exchange for phosphate, sulfate, and thiosulfate, were among these genes. Furthermore, subunits E (ATP5I, MIM 601519) and C1 (ATP5G1, MIM 603192) of the ATP synthase F0 complex F0 were downregulated.

Moreover, we analyzed gene expression data ([25] and Rainer et al. in preparation) obtained for seven T-ALL patients and ten preB-ALL patients with a hyperdiploid genotype for the above mentioned mitochondrial transporters and the gene sets coding for ATP synthase subunits (Table S2). ATP5G1 was repressed by 48% ± 13% in T-ALL patients and 40% ± 15% in B-ALL patients. This supports the hypothesis that GC-reduced energy metabolism may be an important event in therapeutic cell death induction. The patient data concerning SLC25A10
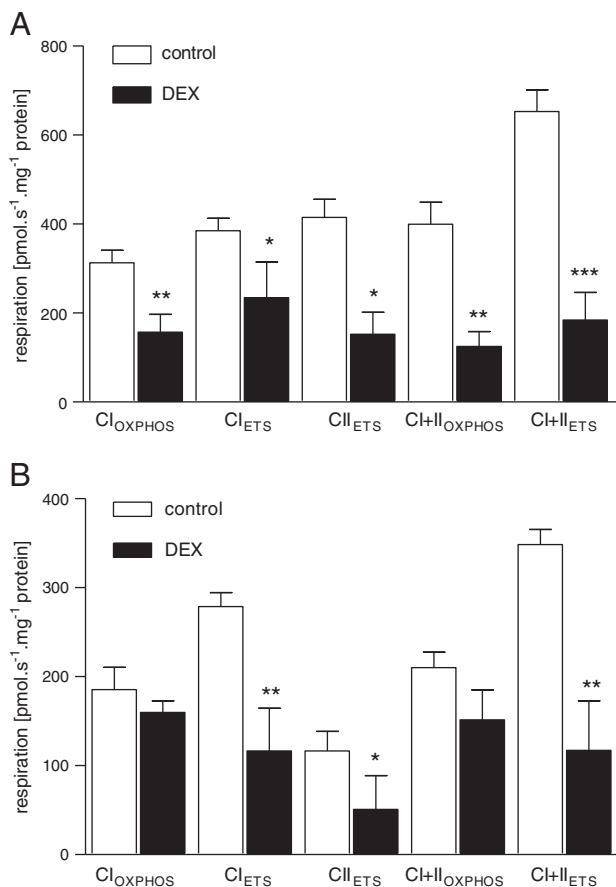
**Table 2**

Downregulation of mitochondrial metabolite transporters and subunits of the ATP synthase.

| Gene name | CEM-CCRF-C7H2 | | NALM-6 | | 697/EU-3 | |
|---|---|---|---|---|---|---|
| | MeanM | Adj $P$ | MeanM | Adj $P$ | MeanM | Adj $P$ |
| ATP5G1 | −1.51 | 6.13E-05[*] | −0.52 | 5.58E-02 | −0.80 | 1.41E-01 |
| ATP5I | −1.11 | 6.72E-03[*] | −0.11 | 7.66E-01 | −0.25 | 7.86E-01 |
| ODC1 | −1.54 | 1.65E-10[*] | −0.56 | 1.25E-03[*] | −0.15 | 7.82E-01 |
| SLC25A10 | −1.55 | 7.37E-04[*] | −0.29 | 4.92E-01 | −0.64 | 1.01E-02[*] |
| SLC25A15 | −1.66 | 4.16E-06[*] | −0.62 | 9.44E-03[*] | −0.84 | 9.50E-04[*] |
| SLC25A19 | −1.75 | 2.14E-07[*] | −0.58 | 8.76E-03[*] | −0.69 | 2.71E-02[*] |
| SLC25A22 | −0.92 | 3.12E-02[*] | −0.49 | 4.90E-02[*] | −0.39 | 3.57E-01 |
| Mean | −1.43 | | −0.45 | | −0.54 | |

Average $\log_2$ fold changes (meanM) and corresponding $P$-values adjusted by the Benjamini–Hochberg method for the GC-sensitive cell lines CEM-CCRF-C7H2, NALM-6, and 697/EU-3, representing extent and significance of regulation after 24 h of treatment with 100 nM dexamethasone. $N = 3$.

[*] $P < 0.05$.

and SLC25A22 showed no consistent downregulation as compared to the cell lines. Nevertheless, either the glutamate or the malate/succinate transporter was reduced in T-ALL and B-ALL patients (Table S2). Since the transporter family SLC25A comprises very low abundant proteins, even a small change could lead to a limitation in mitochondrial substrate supply. Precursor B-ALL patients with ETV6/RUNX1 (previously referred to as TEL/AML1) genotype [7], however, showed on average no change in the expression of these genes (Table S2).

### 3.3.2. Mitochondrial protein translocases

Several mRNA encoding subunits of TIMM and TOMM, which are responsible for uptake and insertion of mitochondrial proteins, were significantly repressed under DEX treatment (Table 3). We measured gene expression levels in 3 different model systems of ALL, the CEM-CCRF-C7H2, 697/EU-3, and the NALM-6 cell line, and found coordinated downregulation, albeit to different extents, of mRNAs for 18 mitochondrial translocase subunits in all 3 cell lines (Table 3). In the T-ALL model (CEM-CCRF-C7H2), 15 of the translocase subunit mRNAs were significantly downregulated (Benjamini–Hochberg adjusted $P < 0.05$). In the precursor B-ALL models, most of the genes did not reach statistical significance; however, there was a trend of repression.

**Table 3**

Downregulation of inner and outer mitochondrial membrane translocases and heat shock protein 70 (HSPA9).

| Gene name | CEM-CCRF-C7H2 | | NALM6 | | 697/EU-3 | |
|---|---|---|---|---|---|---|
| | **MeanM** | **Adj P** | **MeanM** | **Adj P** | **MeanM** | **Adj P** |
| **HSPA9** | -1.10 | 1.73E-08* | -0.67 | 3.37E-03* | -0.66 | 4.20E-02* |
| **TIMM8A** | -0.95 | 1.28E-02* | -0.13 | 4.64E-01 | -0.26 | 4.90E-01 |
| **TIMM8B** | -0.15 | 9.19E-01 | -0.78 | 6.67E-02 | -0.44 | 8.47E-01 |
| **TIMM9** | -1.22 | 3.12E-02* | -0.74 | 1.56E-01 | -0.72 | 4.84E-01 |
| **TIMM10** | -0.91 | 7.60E-02 | -0.37 | 1.76E-01 | -0.62 | 1.34E-01 |
| **TIMM13** | -1.93 | 5.72E-06* | -0.44 | 7.95E-02 | -0.70 | 9.35E-02 |
| **TIMM17A** | -1.07 | 8.71E-03* | -0.62 | 5.19E-02 | -0.54 | 4.18E-01 |
| **TIMM17B** | -0.82 | 4.54E-02* | -0.23 | 3.92E-01 | -0.25 | 6.09E-01 |
| **TIMM22** | -0.68 | 8.57E-04* | 0.09 | 7.06E-01 | -0.40 | 1.47E-01 |
| **TIMM23** | -0.66 | 1.13E-02* | -0.35 | 1.99E-01 | -0.58 | 1.20E-01 |
| **TIMM44** | -1.50 | 4.16E-06* | -0.63 | 1.95E-02* | -0.91 | 2.89E-03* |
| **TIMM50** | -1.18 | 2.44E-07* | -0.30 | 1.47E-01 | -0.74 | 3.93E-03* |
| **TOMM7** | -1.44 | 8.74E-02 | -0.06 | 8.91E-01 | -0.22 | 9.19E-01 |
| **TOMM20** | -0.95 | 4.59E-04* | -0.42 | 1.78E-01 | 0.11 | 9.84E-01 |
| **TOMM22** | -0.70 | 1.44E-02* | -0.17 | 4.00E-01 | -0.24 | 5.89E-01 |
| **TOMM34** | -0.88 | 7.63E-04* | -0.21 | 3.44E-01 | -0.42 | 5.08E-02 |
| **TOMM40** | -1.14 | 1.09E-05* | -0.92 | 1.21E-01 | -0.95 | 9.15E-02 |
| **TOMM40L** | -0.43 | 1.61E-02* | -0.05 | 9.10E-01 | -0.14 | 9.20E-01 |
| **TOMM70A** | -0.77 | 2.59E-03* | -0.57 | 1.59E-02* | -0.23 | 6.89E-01 |
| **mean** | **-0.97** | | **-0.40** | | **-0.47** | |

Average log2 fold changes (meanM) and corresponding $P$-values adjusted by the Benjamini and Hochberg method for the GC-sensitive cell lines CEM-CCRF-C7H2, NALM6, and 697/EU-3, representing extent and significance of regulation after 24 h of treatment with 100 nM dexamethasone. * $P < 0.05$. $N = 3$.
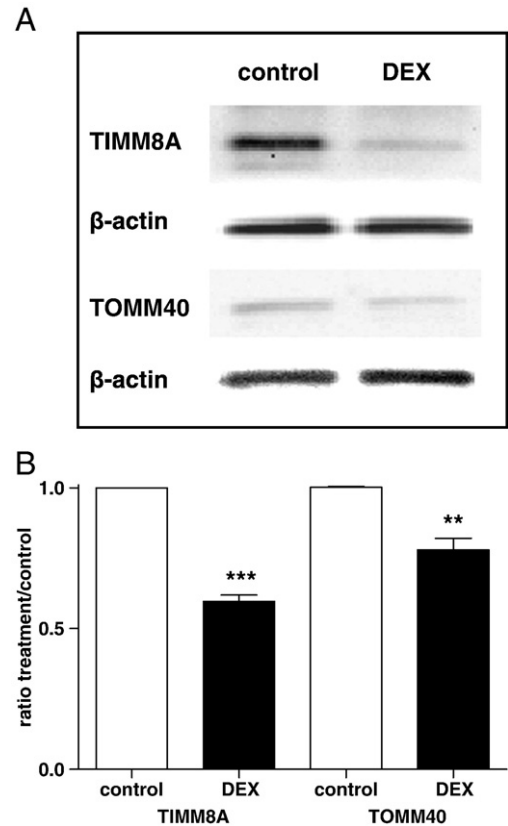


**Fig. 3.** Downregulation of TIMM8A and TOMM40 protein expression in C7H2 cells after 24 h of DEX treatment. Representative Western blots of TIMM8A, TOMM40, and the loading control COX IV (A), and a densitometric analysis of protein bands after imaging by a Molecular Imager® VersaDoc™ MP 4000 system and subsequent integration by Quantity One Software (B) are shown. Volumes of TIMM8A and TOMM40 protein bands were normalized against the loading control and control values were set to 1. (B) Arithmetic means ± SEM and statistical significance compared to controls (**$P < 0.01$, ***$P < 0.001$) are shown. $N = 3$.

Heat shock protein 70 (HSPA9), a mitochondrial chaperone essential for the function of the TIM23 complex, was significantly downregulated in all tested cell lines. During transport of proteins by the TIM23 complex, HSPA9 is recruited by TIMM44. Both genes were repressed nearly to the same extent in all cell lines tested, indicating that the function of TIM23 was strongly reduced. In order to verify our gene expression data, we analyzed protein levels of TIMM8A and TOMM40, which were strongly downregulated at the gene expression level. TIMM8A and TOMM40 also showed a 42% and 25% downregulation, respectively, at the protein level in DEX-treated cells (Fig. 3).

With regard to the TIM and TOM complexes, the ALL patients (T-ALL and precursor B-ALL with hyperdiploidy) showed merely a slight reduction of all analyzed TIMM and TOMM genes and heat shock protein 70 (Table S3). Nevertheless, TIMM8A and TIMM23 were among the 30 most negatively correlated genes with regard to GC bioactivity levels in the serum of T-ALL patients ($N = 4$); thus, high GC serum levels are associated with low expression levels of these two genes and vice versa (Rainer et al., in preparation).

## 4. Discussion

Involvement of mitochondrial alterations and metabolic disturbances have been discussed as important events in GC-induced apoptosis [9,11,26–28] but not studied in detail. Mitochondrial membrane alterations as shown in the present study might contribute to the collapse of vital metabolic pathways, making cells susceptible to apoptosis.

After 24 h of DEX treatment, the observed repression of respiration upon cell membrane permeabilization with digitonin in both GC-sensitive model systems and the detected cytochrome $c$ release in T-ALL cells suggest changes in mitochondrial membrane properties that contribute to apoptosis, possibly via induction of permeability transition.

Digitonin exerts its effect by interaction with cholesterol. The cholesterol content is much lower in mitochondrial compared to plasma membranes; therefore, digitonin concentrations used for plasma membrane permeabilization usually do not affect mitochondrial membranes. A direct effect of digitonin on the mitochondrial membrane cannot be excluded, but it appears unlikely for two reasons: (i) we used a digitonin concentration for plasma membrane permeabilization that was much lower than required for mitochondrial outer membrane permeabilization (we also checked lower concentrations for GC-treated cell, but the effect was the same), and (ii) mitochondrial cholesterol content was not elevated, which would have increased the sensitivity to digitonin (data not shown).

We hypothesize that DEX treatment alters mitochondrial membrane composition, as shown by reduced protein content of two translocases and the strong downregulation of numerous transporters on mRNA level and thus alters mitochondrial membrane properties, making mitochondria more fragile and sensitive to the onset of apoptosis. The importance of the observed phenomena is supported by the fact that none of the GC-resistant ALL model systems tested showed any of these changes. The decreased mitochondrial activity in intact cells after 36 h suggests an accumulation of injuries over time. Changed mitochondrial membrane properties, damage of the respiratory complexes, and/or reduced substrate import could explain the repressed mitochondrial respiratory activity and ATP levels after 36 h of DEX treatment.

Our gene expression data revealed a downregulation of metabolite transporters at the mRNA level. A disturbed substrate transport results in substrate depletion and impairment of different metabolic pathways, e.g. amino acid metabolism, the urea cycle, and mitochondrial respiration [1,29]. Recent data show a strong correlation between disturbed mitochondrial metabolite transport and disease [30]. Disturbed glutamate uptake by its main transporter SLC25A22 results in impairment of the malate/aspartate shuttle and a malfunction of the urea cycle, resulting in reduced nitrogen detoxification. Malate, a metabolite produced in the mitochondrial matrix as well as in the cytoplasm, is taken up by the mitochondria via the dicarboxylate transporter (SLC25A10), which was found to be repressed by DEX treatment. Moreover, we found the mitochondrial C5–C7 oxodicarboxylate carrier SLC25A21 repressed in all cell lines and in 70% of all investigated ALL patients. In addition to the regulation of metabolite transporters, TIMMs and TOMMs were downregulated both at the gene and the protein levels. Except TIMM21, all translocases of the inner mitochondrial membrane are essential for cell viability [31]. A reduction in TIMM and TOMM proteins results in repressed transport and insertion of newly synthesized proteins into mitochondria, which might potentiate the described transcriptional downregulations of the metabolite transporters and the ATP synthase. ATP levels are crucial for cell viability and a reduction is a strong cell death trigger [32]. We reported previously [9] that a moderate reduction in ATP levels by a non-toxic dose of 2-deoxyglucose sensitized cells dramatically to GC. This effect of 2-deoxyglucose on GC-induced cell death could be reverted by the addition of pyruvate and a concomitant increase in ATP in the B-ALL model. In the T-ALL model, pyruvate addition did not result in an increase in ATP levels and the effect of 2-DG on apoptosis could not be reverted.

Patient data revealed strong differences between the response of T- and precursor B-ALL cells to GC treatment and gene expression profiles among ALL patients also showed great variability. Individual patients showed significant regulations in many of the described genes, others no regulation at all, underscoring the need for personalized medical treatment of children suffering from ALL.

The mechanism of GC-induced apoptosis and the phenomenon of GC resistance are still under investigation. In summary, our data provide evidence that alterations in mitochondrial membrane and catalytic properties are an early event in GC-induced metabolic disturbances leading to apoptosis. In contrast, in GC-resistant cells, all tested mitochondrial respiratory parameters remain unchanged, suggesting that a preserved mitochondrial function and membrane properties protect resistant cells against GC-induced metabolic stress. Further support for this hypothesis comes from the transcriptional profiling of GC-resistant T-ALL cell lines, which demonstrated the activation of bioenergetic pathways required for proliferation [11]. This increase may suppress the apoptotic potential and offset the metabolic crisis initiated by GC signaling. In combination with the observations that selective metabolic inhibitors such as 2-deoxyglucose could revert resistance *in vitro* and *ex vivo* in GC-resistant leukemic cells [26] and potentiated the GC effect in GC-sensitive leukemia cells [9], further studies on the role of cellular metabolism and its therapeutic modulation in GC-triggered apoptosis of lymphoblastic leukemia cells are warranted.

## Acknowledgments

## Appendix A. Supplementary data

Supplementary data to this article can be found online at doi:10.1016/j.bbabio.2010.12.010.

## References

[1]  F. Palmieri, The mitochondrial transporter family (SLC25): physiological and pathological implications, Pflügers Arch. Eur. J. Physiol. 447 (2004) 689–709.
[2]  E.R. Kunji, The role and structure of mitochondrial carriers, FEBS Lett. 564 (2004) 239–244.
[3]  S. Sugiyama, S. Moritoh, Y. Furukawa, T. Mizuno, Y.M. Lim, L. Tsuda, Y. Nishida, Involvement of the mitochondrial protein translocator component Tim50 in growth, cell proliferation and the modulation of respiration in drosophila, Genetics 176 (2007) 927–936.
[4]  N. Joza, S.A. Susin, E. Daugas, W.L. Stanford, S.K. Cho, C.Y. Li, T. Sasaki, A.J. Elia, H.Y. Cheng, L. Ravagnan, K.F. Ferri, N. Zamzami, A. Wakeham, R. Hakem, H. Yoshida, Y.Y. Kong, T.W. Mak, J.C. Zuniga-Pflucker, G. Kroemer, J.M. Penninger, Essential role of the mitochondrial apoptosis-inducing factor in programmed cell death, Nature 410 (2001) 549–554.
[5]  L. Scorrano, S.J. Korsmeyer, Mechanisms of cytochrome c release by proapoptotic BCL-2 family members, Biochem. Biophys. Res. Commun. 304 (2003) 437–444.
[6]  M. Dordelmann, A. Reiter, A. Borkhardt, W.D. Ludwig, N. Gotz, S. Viehmann, H. Gadner, H. Riehm, M. Schrappe, Prednisone response is the strongest predictor of treatment outcome in infant acute lymphoblastic leukemia, Blood 94 (1999) 1209–1217.
[7]  C.H. Pui, W.E. Evans, Treatment of acute lymphoblastic leukemia, N. Engl. J. Med. 354 (2006) 166–178.
[8]  R. Kofler, The molecular basis of glucocorticoid-induced apoptosis of lymphoblastic leukemia cells, Histochem. Cell Biol. 114 (2000) 1–7.
[9]  K. Eberhart, K. Renner, I. Ritter, M. Kastenberger, K. Singer, C. Hellerbrand, M. Kreutz, R. Kofler, P.J. Oefner, Low doses of 2-deoxy-glucose sensitize acute lymphoblastic leukemia cells to glucocorticoid-induced apoptosis, Leukemia 23 (2009) 2167–2170.
[10] M.E. Tome, D.B. Johnson, B.K. Samulitis, R.T. Dorr, M.M. Briehl, Glucose 6-phosphate dehydrogenase overexpression models glucose deprivation and sensitizes lymphoma cells to apoptosis, Antioxid. Redox Signal. 8 (2006) 1315–1327.
[11] A.H. Beesley, M.J. Firth, J. Ford, R.E. Weller, J.R. Freitas, K.U. Perera, U.R. Kees, Glucocorticoid resistance in T-lineage acute lymphoblastic leukaemia is associated with a proliferative metabolism, Br. J. Cancer 100 (2009) 1926–1936.

[12] E.M. Strasser-Wozak, R. Hattmannstorfer, M. Hala, B.L. Hartmann, M. Fiegl, S. Geley, R. Kofler, Splice site mutation in the glucocorticoid receptor gene causes resistance to glucocorticoid-induced apoptosis in a human acute leukemic cell line, Cancer Res. 55 (1995) 348–353.

[13] H.W. Findley Jr., M.D. Cooper, T.H. Kim, C. Alvarado, A.H. Ragab, Two new acute lymphoblastic leukemia cell lines with early B-cell phenotypes, Blood 60 (1982) 1305–1309.

[14] S. Schmidt, J.A. Irving, L. Minto, E. Matheson, L. Nicholson, A. Ploner, W. Parson, A. Kofler, M. Amort, M. Erdel, A. Hall, R. Kofler, Glucocorticoid resistance in two key models of acute lymphoblastic leukemia occurs at the level of the glucocorticoid receptor, FASEB J. 20 (2006) 2600–2602.

[15] M. Zhou, L. Gu, F. Li, Y. Zhu, W.G. Woods, H.W. Findley, DNA damage induces a novel p53-survivin signaling pathway regulating cell cycle and apoptosis in acute lymphoblastic leukemia cells, J. Pharmacol. Exp. Ther. 303 (2002) 124–131.

[16] I. Nicoletti, G. Migliorati, M.C. Pagliacci, F. Grignani, C. Riccardi, A rapid and simple method for measuring thymocyte apoptosis by propidium iodide staining and flow cytometry, J. Immunol. Meth. 139 (1991) 271–279.

[17] S. Stadlmann, K. Renner, J. Pollheimer, P.L. Moser, A.G. Zeimet, F.A. Offner, E. Gnaiger, Preserved coupling of oxidative phosphorylation but decreased mitochondrial respiratory capacity in IL-1beta-treated human peritoneal meso-thelial cells, Cell Biochem. Biophys. 44 (2006) 179–186.

[18] E. Gnaiger, Capacity of oxidative phosphorylation in human skeletal muscle: new perspectives of mitochondrial physiology, Int. J. Biochem. Cell Biol. 41 (2009) 1837–1845.

[19] A.V. Kuznetsov, S. Schneeberger, R. Seiler, G. Brandacher, W. Mark, W. Steurer, V. Saks, Y. Usson, R. Margreiter, E. Gnaiger, Mitochondrial defects and heterogeneous cytochrome c release after cardiac cold ischemia and reperfusion, Am. J. Physiol. Heart Circ. Physiol. 286 (2004) H1633–H1641.

[20] D. Pesta, E. Gnaiger, High-resolution respirometry. OXPHOS protocols for human cell cultures and permeabilized fibres from small biopsies of human muscle, in: C. Palmeira, A. Moreno (Eds.), Mitochondrial Bioenergetics: Methods and Protocols, 2010.

[21] J. Rainer, C. Ploner, S. Jesacher, A. Ploner, M. Eduardoff, M. Mansha, M. Wasim, R. Panzer-Grumayer, Z. Trajanoski, H. Niederegger, R. Kofler, Glucocorticoid-regulated microRNAs and mirtrons in acute lymphoblastic leukemia, Leukemia 23 (2009) 746–752.

[22] Z. Wu, R.A. Irizarry, R. Gentleman, F. Martinez-Murillo, F. Spencer, A model-based background adjustment for oligonucleotide expression arrays, J. Am. Stat. Assoc. 99 (2004) 909–918.

[23] G. Smyth, Linear models and empirical Bayes methods for assessing differential expression in microarray experiments, Stat. Appl. Genet. Mol. Biol. 3 (2004) 29.

[24] Y. Benjamini, Y. Hochberg, Controlling the false discovery rate: a practical and powerful approach to multiple testing, J. R. Statist. Soc. B 57 (1995) 289–300.

[25] S. Schmidt, J. Rainer, S. Riml, C. Ploner, S. Jesacher, C. Achmuller, E. Presul, S. Skvortsov, R. Crazzolara, M. Fiegl, T. Raivio, O.A. Janne, S. Geley, B. Meister, R. Kofler, Identification of glucocorticoid-response genes in children with acute lymphoblastic leukemia, Blood 107 (2006) 2061–2069.

[26] E. Hulleman, K.M. Kazemier, A. Holleman, D.J. VanderWeele, C.M. Rudin, M.J. Broekhuis, W.E. Evans, R. Pieters, M.L. den Boer, Inhibition of glycolysis modulates prednisolone resistance in acute lymphoblastic leukemia cells, Blood 113 (2009) 2014–2021.

[27] M.E. Tome, N.W. Lutz, M.M. Briehl, Overexpression of catalase or Bcl-2 delays or prevents alterations in phospholipid metabolism during glucocorticoid-induced apoptosis in WEHI7.2 cells, Biochim. Biophys. Acta 1642 (2003) 149–162.

[28] M.E. Tome, N.W. Lutz, M.M. Briehl, Overexpression of catalase or Bcl-2 alters glucose and energy metabolism concomitant with dexamethasone resistance, Biochim. Biophys. Acta 1693 (2004) 57–72.

[29] M.J. Lindhurst, G. Fiermonte, S. Song, E. Struys, F. De Leonardis, P.L. Schwartzberg, A. Chen, A. Castegna, N. Verhoeven, C.K. Mathews, F. Palmieri, L.G. Biesecker, Knockout of Slc25a19 causes mitochondrial thiamine pyrophosphate depletion, embryonic lethality, CNS malformations, and anemia, Proc. Natl Acad. Sci. USA 103 (2006) 15927–15932.

[30] F. Palmieri, Diseases caused by defects of mitochondrial carriers: a review, Biochim. Biophys. Acta 1777 (2008) 564–578.

[31] D. Mokranjac, W. Neupert, Protein import into mitochondria, Biochem. Soc. Trans. 33 (2005) 1019–1023.

[32] J.M. Garland, A. Halestrap, Energy metabolism during apoptosis. Bcl-2 promotes survival in hematopoietic cells induced to apoptose by growth factor withdrawal by stabilizing a form of metabolic arrest, J Biol. Chem. 272 (1997) 4680–4688.